Comparative proteomic analysis of paclitaxel resistance-related proteins in human breast cancer cell lines

HIROYA FUJIOKA[1], AKIKO SAKAI[2], SATORU TANAKA[1], KOSEI KIMURA[1], AKIKO MIYAMOTO[1], MITSUHIKO IWAMOTO[1] and KAZUHISA UCHIYAMA[1]

[1]Section of Breast and Endocrine Surgery, Department of General and Gastroenterological Surgery; [2]Department of Chemistry, Osaka Medical College, Takatsuki, Osaka 569-8686, Japan

Received May 28, 2015; Accepted October 6, 2016

DOI: 10.3892/ol.2016.5455

Abstract. Paclitaxel is widely used to treat various cancers; however, resistance to this drug is a major obstacle to breast cancer chemotherapy. To identify the proteins involved in paclitaxel resistance, the present study compared the proteomes of MCF-7 human breast cancer cells and its paclitaxel-resistant subclone MCF-7/PTX. Using two-dimensional gel electrophoresis and matrix-assisted laser desorption/ionization time of flight mass spectrometry, 11 upregulated and 12 downregulated proteins were identified in MCF-7/PTX cells compared with the parental cell line. These 23 proteins were functionally classified as stress-induced chaperones, metabolic enzymes and cytoskeletal proteins. The anti-apoptotic proteins, stress-70 protein, 78-kD glucose-regulated protein, peptidyl-prolyl *cis-trans* isomerase A (PPIA) and heterogeneous nuclear ribonucleoprotein H3, were also upregulated in MCF-7/PTX cells. Notably, knockdown of the stress-response chaperone PPIA using small interfering RNA in MCF-7/PTX cells restored their sensitivity to paclitaxel. These findings indicated that PPIA may have an important role in paclitaxel resistance in MCF-7/PTX cells.

Correspondence to: Dr Akiko Sakai, Department of Chemistry, Osaka Medical College, 2-7 Daigaku-machi, Takatsuki, Osaka 569-8686, Japan
E-mail: asakai77777@gmail.com

Dr Kazuhisa Uchiyama, Section of Breast and Endocrine Surgery, Department of General and Gastroenterological Surgery, Osaka Medical College, 2-7 Daigaku-machi, Takatsuki, Osaka 569-8686, Japan
E-mail: uchi@osaka-med.ac.jp

Abbreviations: 5-FU, 5-fluorouracil; GRP78, 78-kD glucose-regulated protein; CK, cytokeratin; HSP7C, heat shock cognate 71-kDa protein; HSPB1, heat shock protein β-1; hnRNP, heterogeneous nuclear ribonucleoprotein; IEF, isoelectric focusing; MALDI, matrix-assisted laser desorption/ionization; PPIA, peptidyl-prolyl *cis-trans* isomerase A; PKM2, pyruvate kinase M2; GRP75, stress-70 protein; SODC, superoxide dismutase [Cu-Zn]; 2-DE, two-dimensional gel electrophoresis; TOF, time of flight; UGDH, UDP-glucose 6-dehydrogenase

Key words: paclitaxel resistance, proteomics, proteome, breast cancer, peptidyl-prolyl *cis-trans* isomerase A

Introduction

Taxanes, including paclitaxel and docetaxel, are microtubule-stabilizing agents that are widely used to treat various cancers. Taxane-resistant breast cancer is common; therefore, the identification of resistance markers and a detailed understanding of the mechanisms mediating paclitaxel resistance are required to develop optimal treatment strategies and to identify responsive patients (1). A previous study described at least three potential mechanisms of paclitaxel resistance (2). The first involves decreased intracellular drug accumulation caused by the overexpression of membrane-bound drug efflux proteins, such as P-glycoprotein. However, clinical trials focusing on P-glycoprotein inhibitors as chemosensitizing agents did not report promising outcomes for patients with relapsing solid tumors and hematological malignancies (3). The other two mechanisms involve mutations in β-tubulin and overexpression of β-tubulin isotypes (2). For example, numerous studies reported that mutations in the paclitaxel-binding sites of β-tubulin were associated with drug resistance, while other studies were unable to detect these mutations in paclitaxel-resistant breast cancers (4-7). Overexpression of β-tubulin isotypes occurs in a restricted number of patients with paclitaxel-resistant ovarian cancer and occasionally in patients with breast cancer; however, knockdown of β-tubulin expression by RNA interference had no effect on the sensitivity of paclitaxel-resistant ovarian cancer cells (6,8,9). Therefore, the proposed mechanisms of paclitaxel resistance remain controversial.

Global analysis of gene expression using cDNA microarray is often used to determine the molecular mechanisms underlying drug resistance. Since the correlation between mRNA abundance and protein levels is poor, proteome analysis is considered superior to cDNA microarrays for the analysis of cell function. Furthermore, two-dimensional gel electrophoresis (2-DE) analysis offers advantages because of its high resolution and ability to detect posttranslational modifications (10,11). Therefore, a proteomic approach using 2-DE in combination with drug sensitivity studies may provide further insight into the mechanisms of paclitaxel resistance.

In the present study, a proteomic analysis using 2-DE and matrix-assisted laser desorption/ionization (MALDI)-time of flight (TOF) mass spectrometry was conducted to identify proteins that play critical roles in paclitaxel resistance. The proteomic analysis revealed 11 upregulated and 12 down-regulated proteins in paclitaxel-resistant MCF-7/PTX cells compared with the paclitaxel-sensitive MCF-7 parental cells. Furthermore, it was demonstrated that peptidyl-prolyl *cis-trans* isomerase A (PPIA), which is also known as cyclophilin A, may have an important role in the resistance of tumor cells to paclitaxel.

Materials and methods

Cell culture. The human breast cancer cell line MCF-7 and its paclitaxel-resistant subclone MCF-7/PTX were obtained from Dr Amadeo M. Parissenti (Tumor Biology Research Program, Sudbury Regional Hospital, Sudbury, Canada) (12). Cells were cultured in Dulbecco's modified Eagle's medium (Wako Pure Chemical Industries, Ltd., Osaka, Japan) supplemented with 10% fetal bovine serum (Tissue Culture Biologicals, Long Beach, CA, USA) at 37˚C in a humidified atmosphere containing 5% CO_2, and were harvested in mid-log phase.

MTT assays for drug sensitivity. Cell viability was assessed 3 days later using MTT assays, as described previously (13). The cells ($5x10^3$ per well) were seeded into 96-well culture plates and pre-incubated for 24 h at 37˚C. Paclitaxel was added at various concentrations (0, 0.1, 0.3, 1, 3, 10, 30, 100, 300 and 1000 nM) and then incubated for 3 days at 37˚C. MTT solution was added (final concentration, 0.45 μg/ml) and subsequently incubated for 2 h at 37˚C. MTT formazan crystals were dissolved in DMSO (Nacalai Tesque, Inc., Kyoto, Japan). The absorbance of each well was read at 540 mn using a SH-1000Lab microplate reader (Corona Electric Co., Ltd., Hitachinaka, Japan). Half maximal inhibitory concentration (IC_{50}) values were calculated from three independent experiments performed in triplicate. The results are shown as a percentage of the absorbance of the medium alone, and are expressed as the mean ± standard error of the mean.

Protein preparation. Harvested cells were washed in ice-cold PBS prior to lysing in chilled lysis buffer containing 7 M urea (Invitrogen; Thermo Fisher Scientific, Inc., Waltham, MA, USA), 2 M thiourea, 5% (w/v) CHAPS, 5% (v/v) IPG buffer (pH 3-10 NL; GE Healthcare Life Sciences, Chalfont, UK), 50 mM DTT and 25 μg/ml each of DNase I and RNase A (Sigma-Aldrich; Merck Millipore, Darmstadt, Germany). Lysates were sonicated three times for 3 sec each (Handy Sonic UR-20P; Tomy Seiko, Tokyo, Japan). Samples were centrifuged at 15,000 x *g* for 30 min, and the supernatants were subjected to protein quantification using a 2-D quantification kit (GE Healthcare Life Sciences) prior to use in the 2-DE experiments.

2-DE experiments. 2-DE was performed as described previously (14). For isoelectric focusing (IEF), an Immobiline DryStrip (pH 4-7 or 3-10, 7 cm; GE Healthcare Life Sciences) was immersed in sample solution (~500 μg of protein) and rehydration buffer (8 M urea, 0.5% [w/v] CHAPS, 20 mM DTT and 1.25% [v/v] IPG buffer). IEF was performed using the NA-1410R7 electrophoresis apparatus (Nihon Eido, Co., Ltd., Tokyo, Japan) set to 50 V for 6 h, 100 V for 6 h and 2,000 V for 7-9 h. Subsequently, the IPG strips were equilibrated at room temperature for 15 min in a solution containing 6 M urea, 1% SDS, 30% glycerol, 50 mM Tris-HCl (pH 8.8), and 60 mM DTT. The strips were equilibrated for an additional 15 min in the same solution, except that DTT was replaced with 0.24 M iodoacetamide, prior to 2-D SDS-PAGE using 12.5% SDS gels. After electrophoresis, the gels were fixed in 10% trichloroacetic acid solution for 1.5 h, washed with double-distilled water three times for 5 min each, stained with Coomassie brilliant blue (CBB) R-250, and then scanned using a GS-800 Calibrated Densitometer (Bio-Rad Laboratories, Inc., Hercules, CA, USA). To verify the results, lysates from three individual preparations were run on four pH 4-7 and pH 3-10 NL gels each.

Image analysis. The 2-DE images were analyzed using Prodigy 2D software (version 1; Nonlinear Dynamics, Ltd., Durham, NC, USA). Spots were detected, matched automatically to a master gel and then edited manually. The total intensity of valid spots was used for normalization. Matched spots from triplicate gel sets with a statistically significant difference in intensities ($P<0.05$) and an average fold difference of >1.5 in spot volume were defined as differentially expressed between MCF-7 and MCF-7/PTX cells.

In-gel digestion. A pipette tip was used to excise protein spots from the 2-DE gels. Gel pieces were destained in a solution containing 30% acetonitrile and 25 mM ammonium bicarbonate for 10 min, dehydrated in 100% acetonitrile for 10 min, and then dried using a SpeedVac (Tomy Seiko). Dried gel pieces were rehydrated for 30 min on ice in 5 μl of 50 mM ammonium bicarbonate containing 50 ng of sequencing-grade modified trypsin (Promega Corporation, Madison, WI, USA). After overnight incubation at 37˚C, peptides were extracted by vortexing for 30 min followed by sonicating for 3 min.

Protein identification by mass spectrometry. The peptide extracts were desalted using C18 ZipTips (Merck Millipore). Mass spectrometry was performed using an Ultraflex II TOF/TOF mass spectrometer (Bruker Corporation, Billerica, MA, USA) with an accelerating voltage of 20 kV, and spectra were externally calibrated using the peptide calibration standard II (Bruker Corporation). Proteins were identified by matching the peptide mass fingerprinting and TOF/TOF results with the Swiss-Prot database (http://www.uniprot.org/) using the MASCOT Search engine v.2.2 (Matrix Science Ltd., London, UK). Database searches were performed using the following parameters: Taxonomy, *Homo sapiens*; and enzyme, trypsin. One missed cleavage was allowed. Carbamidomethylation was selected as a fixed modification and methionine oxidation was allowed as a variable. The peptide and fragment mass tolerances were set to 50 or 100 ppm and 0.5 Da, respectively.

Transfection of MCF-7/PTX cells with a PPIA-specific small interfering (si)RNA. Cells were transfected with Silencer Select Pre-designed siRNA specific for PPIA (s198123; Ambion;

Table I. Identification of upregulated proteins in MCF-7/PTX cells compared with MCF-7 cells.

No.	Protein name	Locus name	Mr (Da)[a]	pI[b]	Mascot score[c]	Fold change
1	Stress-70 protein, mitochondrial	GRP75	73,920	5.87	233	1.9
2	Stress-70 protein, mitochondrial	GRP75	73,920	5.87	240	1.7
3	Heterogeneous nuclear ribonucleoprotein H3	HNRH3	36,960	6.37	172	1.7
4	Heat shock cognate 71 kDa protein	HSP7C	71,082	5.37	124	2.4
5	Heat shock cognate 71 kDa protein	HSP7C	71,082	5.37	126	2.5
6	Pyruvate kinase M1/M2	KPYM	58,470	7.96	148	1.9
7	Stathmin	STMN1	17,292	5.76	127	1.5
8	Peptidyl-prolyl *cis-trans* isomerase A	PPIA	18,229	7.68	124	1.5
9	ATP synthase β-subunit	ATPB	56,525	5.26	216	1.7
10	Tropomyosin α-1 chain	TPM1	32,746	4.69	146	1.8
11	Nucleoside diphosphate kinase A	NDKA	17,309	5.83	122	1.7
12	Superoxide dismutase [Cu-Zn]	SODC	16,154	5.7	168	1.5
13	78 kD glucose-regulated protein	GRP78	72,402	5.07	161	2.4

[a]Theoretical molecular mass (Da) and [b]pI were obtained from the Swiss-Prot database. [c]Mascot scores were based on the combined mass and mass/mass spectra from matrix-assisted laser desorption/ionization-TOF/TOF identification. pI, isoelectric point; TOF, time of flight.

Thermo Fisher Scientific, Inc.) at a final concentration of 5 nM. Transfections were performed in six-well plates using Lipofectamine RNAiMAX (Invitrogen; Thermo Fisher Scientific, Inc.), according to the manufacturer's protocol. Silencer Select negative control siRNA #1 (Invitrogen; Thermo Fisher Scientific, Inc.) was used as a negative control. Gene silencing was assessed between 24 and 72 h following transfection by western blotting.

Western blotting. Cells were lysed using Cell Lysis Buffer M containing 20 mM Tris-HCl (pH 7.4), 200 mM NaCl, 0.05% Nonidet P-40, and 2.5 mM $MgCl_2$ (Wako Pure Chemical Industries, Ltd.). Lysates were sonicated for 3 sec on ice and then centrifuged at 15,000 x *g* for 15 min at 4˚C. Protein concentration was determined using the Quick Start Bradford Protein assay (Bio-Rad Laboratories, Inc.) and protein samples (10 μg/lane) were separated by 15% SDS-PAGE followed by semidry transfer to a polyvinylidene difluoride (PVDF) membrane (GE Healthcare Life Sciences). The membrane was blocked with 3% membrane blocking agent (GE Healthcare Life Sciences) in PBS containing 0.1% Tween-20 (PBS-Tween), incubated for 1 h at room temperature with an anti-PPIA antibody (1:7,500 dilution; cat. no. 07-313; Merck Millipore) in 3% membrane blocking agent in PBS-Tween for 2 h, and incubated further with a horseradish peroxidase-conjugated species-specific donkey antibody (1:50,000 dilution; cat. no. NA934V; GE Healthcare Life Sciences). Immunoreactive bands were visualized using an ECL Prime detection kit and Hyperfilm ECL (GE Healthcare Life Sciences). The films were scanned with the GS-800 Calibrated Densitometer and analyzed by Quantity One, version 4.5.0. software (Bio-Rad Laboratories, Inc.). In parallel, the blotted PVDF membranes were stained with 0.008% Direct Blue 71 (Sigma-Aldrich; Merck Millipore) as described previously (15), analyzed by the GS-800 and Quantity One software version 4.5.0 (Bio-Rad Laboratories, Inc.), and the total protein intensity of each lane was used as the sample loading control, as described previously (16).

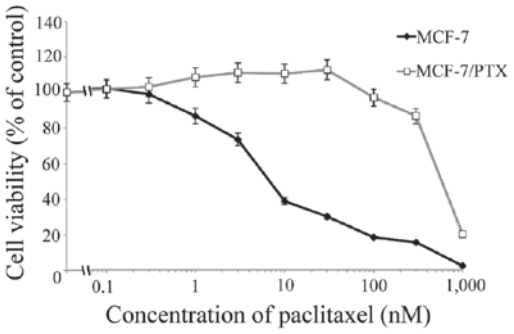

Figure 1. Effects of paclitaxel on the viability in MCF-7 and MCF-7/PTX cells. Cells were treated with paclitaxel for 74 h and cell viability was analyzed by MTT assays. The results are shown as the percentage of absorbance of the medium alone, and are expressed as the mean ± standard error of the mean of three independent experiments.

Statistical analysis. Statistical analyses were performed using Excel 2010 (Microsoft Corporation, Redmond, WA, USA). The results are expressed as the mean ± standard error of the mean, and $P<0.05$ was considered to indicate a statistically significant difference.

Results

Paclitaxel resistance in human breast cancer cell lines. The cytotoxicity of paclitaxel on the human breast cancer cell line MCF-7 and its paclitaxel-resistant subclone MCF-7/PTX was compared using MTT assays (Fig. 1). The IC_{50} values for paclitaxel were 7.7±1.5 and 580±50 nM for MCF-7 and MCF-7/PTX cells, respectively ($P<0.05$). The cytotoxicity of paclitaxel on MCF-7/PTX cells was 75-fold lower than its cytotoxicity on MCF-7 cells.

Identification of differentially expressed proteins. The protein expression profiles of the MCF-7 and MCF-7/PTX cells were

Table II. Identification of downregulated proteins in MCF-7/PTX cells compared with MCF-7 cells.

No.	Protein name	Locus name	Mr (Da)[a]	pI[b]	Mascot score[c]	Fold change
14	Glucose-6-phosphate 1-dehydrogenase	G6PD	59,675	6.39	187	0.67
15	26S protease regulatory subunit 7	PRS7	49,002	5.71	181	0.67
16	UDP-glucose 6 dehydrogenase	UGDH	55,674	6.73	258	0.33
17	UDP-glucose 6 dehydrogenase	UGDH	55,674	6.73	233	0.34
18	Phosphoglycerate mutase 1	PGAM1	28,900	6.67	116	0.67
19	Peroxiredoxin-6	PRDX6	27,838	6.28	116	0.63
20	Tubulin β-4B chain	TBB4B	50,255	4.79	132	0.59
21	Peroxiredoxin-1	PRDX1	22,324	8.27	185	0.67
22	Cytokeratin 8	K2C8	53,671	5.52	307	0.67
23	Cytokeratin 8	K2C8	53,671	5.52	323	0.56
24	Cytokeratin 8	K2C8	53,671	5.52	199	0.36
25	Tubulin α-1A chain	TBA1A	50,788	4.94	140	0.67
26	Heat shock protein β-1	HSPB1	22,826	5.98	153	0.43
27	Heat shock protein β-1	HSPB1	22,826	5.98	123	0.71
28	Heat shock protein β-1	HSPB1	22,826	5.98	104	0.42
29	Actin, cytoplasmic 1	ACTB	42,052	5.29	81	0.53
30	Cytokeratin 18	K1C18	48,629	5.34	208	0.67

[a]Theoretical molecular mass (Da) and [b]pI were obtained from the Swiss-Prot database. [c]Mascot scores were based on the combined mass and mass/mass spectra from matrix-assisted laser desorption/ionization-TOF/TOF identification. pI, isoelectric point; TOF, time of flight.

compared to identify proteins associated with paclitaxel sensitivity. To confirm reproducibility, proteins were extracted from each cell line three times and four 2-D gels were prepared for each cell extract. Gel analysis showed a consistent image with reproducible resolution of the 2-DE maps. CBB R-250 staining revealed >400 protein spots on each 7-cm gel (pH 3-10 NL) (Fig. 2C and D). Six and seven images were analyzed for the pH 3-10 and pH 4-7 gels, respectively.

Differences in protein expression that were ≥1.5-fold ($P<0.05$), as indicated by changes in the intensity of the spots on the gels, were defined as statistically significant (Fig. 2). In total, 30 differentially expressed protein spots were detected, including 13 upregulated and 17 downregulated spots. Using this procedure, 11 proteins were identified as upregulated, while 12 proteins were determined to be downregulated (Tables I and II). The functions of identified proteins were assigned using information from the Swiss-Prot database (www.uniprot.org/uniprot/) and the protein function databases Pfam (pfam.xfam.org/).

Knockdown of PPIA expression in MCF-7/PTX cells. PPIA expression was significantly higher in MCF-7/PTX cells compared with MCF-7 cells (Fig. 2C and D, spot no. 8). To investigate the role of PPIA in paclitaxel resistance, siRNA-mediated knockdown of PPIA was performed and paclitaxel-induced cell death was assessed by viability assays (Fig. 3A). Notably, paclitaxel sensitivity was significantly increased in siRNA-treated cells compared with untransfected MCF-7/PTX cells and negative control siRNA-treated counterparts (Fig. 3B). The IC_{50} values of paclitaxel were 3.2±1.1, 160±57, 175±100 and 14±9 nM in MCF-7 cells, MCF-7/PTX cells, negative control siRNA transfected MCF-7/PTX cells and PPIA-siRNA-transfected MCF-7/PTX cells, respectively. These results indicate a close association between PPIA and paclitaxel resistance in MCF-7 cells, and suggest that PPIA levels may predict MCF-7 resistance to paclitaxel.

Discussion

The purpose of this study was to investigate the mechanisms underlying paclitaxel resistance in breast cancer cells and to identify markers of drug resistance. To this end, a proteomic analysis using 2-DE coupled with MALDI-TOF/TOF mass spectrometry was conducted, and 23 differentially expressed proteins between paclitaxel-resistant MCF-7/PTX cells and parental MCF-7 cells were identified. These proteins were classified into several functional groups, including roles in the stress response, metabolism, cytoskeleton and apoptosis. Differences between the experimental and theoretical molecular mass/isoelectric point values were observed for stress-70 protein (GRP75), heat shock cognate 71-kDa protein (HSP7C), UDP-glucose 6 dehydrogenase (UGDH), cytokeratin 8 (CK8) and heat shock protein β-1 (HSPB1), which may be attributed to posttranslational modifications such as cleavage and/or phosphorylation.

Notably, it was observed that the stress-response chaperones, GRP75, HSP7C, 78-kD glucose-regulated protein (GRP78), PPIA and superoxide dismutase [Cu-Zn] (SODC) were upregulated in MCF-7/PTX cells, whereas 26S protease regulatory subunit 7, peroxiredoxin-1, peroxiredoxin-6 and HSPB1 were downregulated in MCF-7/PTX cells. GRP75, HSP7C and GRP78 are members of the heat shock protein 70 (HSP70) superfamily, which perform essential

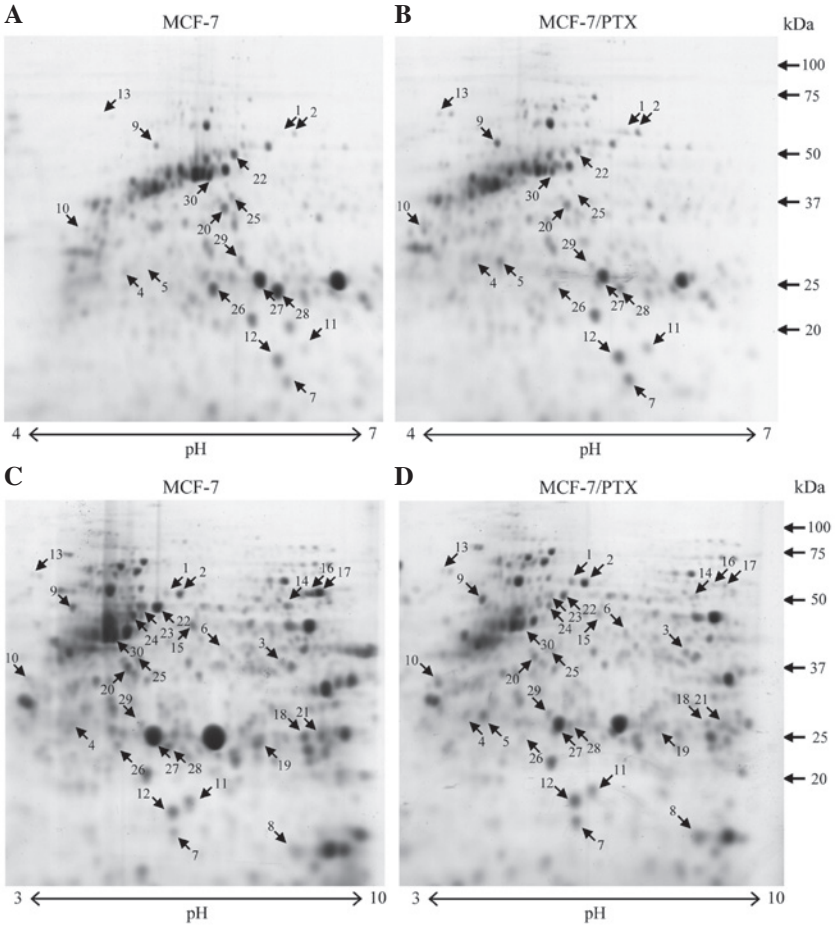

Figure 2. Two-dimensional gel electrophoresis maps of MCF-7 and MCF-7/PTX cells. Total protein extracts prepared from MCF-7 and MCF-7/PTX were separated on (A and B) pH 4-7, 7-cm IPG strips (C and D) pH 3-10 NL, 7-cm IPG strips, followed by 12.5% SDS-PAGE and staining with Coomassie brilliant blue R-250. Numbers refer to the proteins listed in Tables I and II.

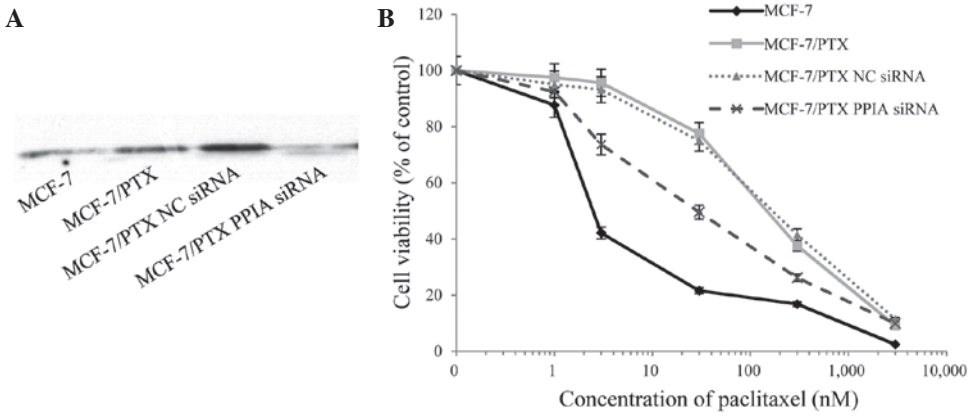

Figure 3. Effects of PPIA knockdown by siRNA on paclitaxel resistance in MCF-7/PTX cells. (A) Western blot analysis of PPIA in MCF-7 and MCF-7/PTX cells 3 days after siRNA transfection. The blotted membranes were stained, and the total protein intensity of each lane was used as the sample loading control. (B) The viability of cells transfected with PPIA siRNA was assessed by MTT assays 3 days after transfection. Viability is shown as the percentage of absorbance of the medium alone in MCF-7, MCF-7/PTX, negative control (NC) siRNA-transfected MCF-7/PTX and PPIA-siRNA-transfected MCF-7/PTX cells. Data are expressed as the mean ± standard error of the mean of three independent experiments. NC, negative control; PPIA, peptidyl-prolyl *cis-trans* isomerase A; siRNA, small interfering RNA.

roles in facilitating proper protein folding and in preventing the aggregation of denatured proteins in order to maintain protein homeostasis (17). These proteins are upregulated by heat, hypoxia, oxidative stress and toxic chemicals, and subsequently enhance cell survival (17). HSP70 family members are highly expressed by cancer cells, wherein they promote cell growth and survival via multiple anti-apoptotic functions (17). For instance, GRP75 overexpression has been associated with increased cancer cell malignancy, implicating its use as a biomarker of metastatic cancer (18,19).

Furthermore, knockdown of endogenous GRP78 expression by siRNA sensitized human breast cancer cells to estrogen starvation-induced apoptosis (20), while its upregulation is associated with resistance to chemotherapeutic drugs such as doxorubicin, 5-fluorouracil (5-FU) and vincristine (21). In addition, SODC eliminates reactive oxygen species and promotes cisplatin resistance in ovarian cancer cells (22). The authors of the present study hypothesize that these proteins may also function as anti-apoptotic factors in MCF-7/PTX cells and may play a role in paclitaxel resistance.

The present study demonstrated that PPIA was upregulated in paclitaxel-resistant breast cancer cells, and that its siRNA-mediated knockdown restored paclitaxel sensitivity to MCF-7/PTX cells. PPIA is a peptidyl-prolyl *cis-trans* isomerase that catalyzes the *cis-trans* isomerization of proline imidic peptide bonds, promotes protein folding and binds to the immunosuppressive drug cyclosporin A (23). A previous study reported that PPIA is overexpressed in many cancers and is involved in the various stages of tumorigenesis (24). Furthermore, PPIA upregulation was shown to prevent cisplatin-induced apoptosis by limiting the subsequent accumulation of reactive oxygen species, while PPIA knockdown increased the rate of cell death (25). Therefore, we hypothesized that PPIA functions in the regulation of cell death and paclitaxel resistance in MCF-7/PTX cells. In future studies, we plan to investigate whether PPIA is a prognostic biomarker for paclitaxel resistance using clinical tumor specimens.

The present study demonstrated that three metabolic proteins, pyruvate kinase M2 (PKM2), ATP synthase β and nucleoside diphosphate kinase A, were upregulated, whereas glucose-6-phosphate 1-dehydrogenase, UGDH and phosphoglycerate mutase 1 were downregulated, in MCF-7/PTX cells. Notably, the differential expression of PKM2 (26) and ATP synthase β (27) has been shown to have important roles in multi-drug resistance and apoptosis. Furthermore, heterogeneous nuclear ribonucleoprotein (hnRNP) H3 (HNRH3), which is a member of the hnRNP protein family that includes numerous nucleic acid binding proteins and spliceosome components and which function in the splicing of selected target mRNAs (28), has been shown to prevent the apoptosis of cancer cells by regulating the alternative splicing of transcripts that have important roles in apoptosis (29). Therefore, the upregulation of certain anti-apoptotic proteins in MCF-7/PTX cells may also prevent apoptosis induced by paclitaxel.

The present study also demonstrated the upregulation of the cytoskeletal proteins, stathmin and tropomyosin α-1, and the downregulation of tubulin α-1A, tubulin β-4B, β-actin, CK8 and CK18, in MCF-7/PTX cells. In our previous study, it was demonstrated that CK8 undergoes differential phosphorylation and/or cleavage in 5-FU-resistant colon cancer cell lines (14). Similarly, in the present study, full length 53-kDa CK8 (Fig. 2, spots no. 22 and 23) and its 50-kDa cleavage product (Fig. 2, spot no. 24) were downregulated in paclitaxel-resistant cells. CK8 and CK18 function in the cytoskeleton as intermediate filament components, and are phosphorylated in response to cellular stress (30). Furthermore, cleaved, soluble fragments of CK released from apoptotic cancer cells can be detected in bodily fluids, including serum (31). Therefore, we plan to analyze clinical samples in future studies to determine whether the phosphorylated and/or cleaved forms of CK8 and CK18 are potential prognostic biomarkers for paclitaxel and 5-FU resistance.

Stathmin is a microtubule-destabilizing protein and plays an important role in the regulation of mitosis (32). Previous studies have determined that stathmin expression is associated with paclitaxel resistance in breast cancer cell lines (33) and with clinical responses to taxanes in patients receiving standard treatment (34). Notably, stathmin and the stress-response chaperones, GRP75 and GRP78, bind to tubulin (35), which is the target of paclitaxel. Among the 14 identified tubulin heterodimer-associated proteins, GRP75, GRP78 and stathmin were all upregulated in MCF-7/PTX cells. This may be the result of direct or indirect effects on paclitaxel resistance and/or stress-response chaperones, which could convey protection against paclitaxel-induced stress and apoptosis.

In conclusion, the present study identified 23 proteins that were differentially expressed in paclitaxel-resistant MCF-7/PTX cells compared with the paclitaxel-sensitive parental MCF-7 cell line using proteomic techniques. Among these proteins, PPIA levels were upregulated in MCF-7/PTX cells, the knockdown of which restored paclitaxel resistance. These results suggested that PPIA plays an important role in paclitaxel resistance in MCF-7/PTX cells, likely by inhibiting apoptosis through various means.

Acknowledgements

This study was supported by JSPS KAKENHI (grant nos. 23510267 and 25870924). This manuscript was prepared with the assistance of a scientific editing service.

References

1. Tan M and Yu D: Molecular mechanisms of erbB2-mediated breast cancer chemoresistance. Adv Exp Med Biol 608: 119-129, 2007.
2. Kavallaris M: Microtubules and resistance to tubulin-binding agents. Nat Rev Cancer 10: 194-204, 2010.
3. Pusztai L, Wagner P, Ibrahim N, Rivera E, Theriault R, Booser D, Symmans FW, Wong F, Blumenschein G, Fleming DR, *et al*: Phase II study of tariquidar, a selective P-glycoprotein inhibitor, in patients with chemotherapy-resistant, advanced breast carcinoma. Cancer 104: 682-691, 2005.
4. Katsetos CD, Herman MM and Mörk SJ: Class III beta-tubulin in human development and cancer. Cell Motil Cytoskeleton 55: 77-96, 2003.
5. Lee KM, Cao D, Itami A, Pour PM, Hruban RH, Maitra A and Ouellette MM: Class III beta-tubulin, a marker of resistance to paclitaxel, is overexpressed in pancreatic ductal adenocarcinoma and intraepithelial neoplasia. Histopathology 51: 539-546, 2007.
6. Sève P and Dumontet C: Is class III beta-tubulin a predictive factor in patients receiving tubulin-binding agents? Lancet Oncol 9: 168-175, 2008.
7. Katsetos CD, Dráberová E, Legido A, Dumontet C and Dráber P: Tubulin targets in the pathobiology and therapy of glioblastoma multiforme. I. Class III beta-tubulin. J Cell Physiol 221: 505-513, 2009.
8. Kavallaris M, Kuo DY, Burkhart CA, Regl DL, Norris MD, Haber M and Horwitz SB: Taxol-resistant epithelial ovarian tumors are associated with altered expression of specific beta-tubulin isotypes. J Clin Invest 100: 1282-1293, 1997.
9. Gan PP, Pasquier E and Kavallaris M: Class III beta-tubulin mediates sensitivity to chemotherapeutic drugs in non small cell lung cancer. Cancer Res 67: 9356-9363, 2007.
10. Wilhelm M, Schlegl J, Hahne H, Gholami AM, Lieberenz M, Savitski MM, Ziegler E, Butzmann L, Gessulat S, Marx H, et al: Mass-spectrometry-based draft of the human proteome. Nature 509: 582-587, 2014.

11. Sá-Correia I and Teixeira MC: 2D electrophoresis-based expression proteomics: A microbiologist's perspective. Expert Rev Proteomics 7: 943-953, 2010.
12. Villeneuve DJ, Hembruff SL, Veitch Z, Cecchetto M, Dew WA and Parissenti AM: cDNA microarray analysis of isogenic paclitaxel- and doxorubicin-resistant breast tumor cell lines reveals distinct drug-specific genetic signatures of resistance. Breast Cancer Res Treat 96: 17-39, 2006.
13. Carmichael J, DeGraff WG, Gazdar AF, Minna JD and Mitchell JB: Evaluation of a tetrazolium-based semiautomated colorimetric assay: Assessment of chemosensitivity testing. Cancer Res 47: 936-942, 1987.
14. Sakai A, Otani M, Miyamoto A, Yoshida H, Furuya E and Tanigawa N: Identification of phosphorylated serine-15 and -82 residues of HSPB1 in 5-fluorouracil-resistant colorectal cancer cells by proteomics. J Proteomics 75: 806-818, 2012.
15. Aldridge GM, Podrebarac DM, Greenough WT and Weiler IJ: The use of total protein stains as loading controls: an alternative to high-abundance single-protein controls in semi-quantitative immunoblotting. J Neurosci Methods 172: 250-254, 2008.
16. Hong HY, Yoo GS and Choi JK: Direct Blue 71 staining of proteins bound to blotting membranes. Electrophoresis 21: 841-845, 2000.
17. Murphy ME: The HSP70 family and cancer. Carcinogenesis 34: 1181-1188, 2013.
18. Yi X, Luk JM, Lee NP, Peng J, Leng X, Guan XY, Lau GK, Beretta L and Fan ST: Association of mortalin (HSPA9) with liver cancer metastasis and prediction for early tumor recurrence. Mol Cell Proteomics 7: 315-325, 2008.
19. Rozenberg P, Kocsis J, Saar M, Prohászka Z, Füst G and Fishelson Z: Elevated levels of mitochondrial mortalin and cytosolic HSP70 in blood as risk factors in patients with colorectal cancer. Int J Cancer 133: 514-518, 2013.
20. Fu Y, Li J and Lee AS: GRP78/BiP inhibits endoplasmic reticulum BIK and protects human breast cancer cells against estrogen starvation-induced apoptosis. Cancer Res 67: 3734-3740, 2007.
21. Roller C and Maddalo D: The molecular chaperone GRP78/BiP in the development of chemoresistance: Mechanism and possible treatment. Front Pharmacol 4: 10, 2013.
22. Kim JW, Sahm H, You J and Wang M: Knock-down of superoxide dismutase 1 sensitizes cisplatin-resistant human ovarian cancer cells. Anticancer Res 30: 2577-2581, 2010.
23. Obchoei S, Wongkhan S, Wongkham C, Li M, Yao Q and Chen C: Cyclophilin A: Potential functions and therapeutic target for human cancer. Med Sci Monit 15: RA221-RA232, 2009.
24. Nigro P, Pompilio G and Capogrossi MC: Cyclophilin A: A key player for human disease. Cell Death Dis 4: e888, 2013.
25. Choi KJ, Piao YJ, Lim MJ, Kim JH, Ha J, Choe W and Kim SS: Overexpressed cyclophilin A in cancer cells renders resistance to hypoxia- and cisplatin-induced cell death. Cancer Res 67: 3654-3662, 2007.
26. Pandita A, Kumar B, Manvati S, Vaishnavi S, Singh SK and Bamezai RN: Synergistic combination of gemcitabine and dietary molecule induces apoptosis in pancreatic cancer cells and down regulates PKM2 expression. PLoS One 9: e107154, 2014.
27. Xiao X, Yang J, Li R, Liu S, Xu Y, Zheng W, Yi Y, Luo Y, Gong F, Peng H, *et al*: Deregulation of mitochondrial ATPsyn-β in acute myeloid leukemia cells and with increased drug resistance. PLoS One 8: e83610, 2013.
28. Dreyfuss G, Kim VN and Kataoka N: Messenger-RNA-binding proteins and the messages they carry. Nat Rev Mol Cell Biol 3: 195-205, 2002.
29. Rauch J, O'Neill E, Mack B, Matthias C, Munz M, Kolch W and Gires O: Heterogeneous nuclear ribonucleoprotein H blocks MST2-mediated apoptosis in cancer cells by regulating A-Raf transcription. Cancer Res 70: 1679-1688, 2010.
30. Liao J, Ku NO and Omary MB: Stress, apoptosis, and mitosis induce phosphorylation of human keratin 8 at Ser-73 in tissues and cultured cells. J Biol Chem 272: 17565-17573, 1997.
31. Barak V, Goike H, Panaretakis KW and Einarsson R: Clinical utility of cytokeratins as tumor markers. Clin Biochem 37: 529-540, 2004.
32. Rubin CI and Atweh GF: The role of stathmin in the regulation of the cell cycle. J Cell Biochem 93: 242-250, 2004.
33. Alli E, Yang JM, Ford JM and Hait WN: Reversal of stathmin-mediated resistance to paclitaxel and vinblastine in human breast carcinoma cells. Mol Pharmacol 71: 1233-1240, 2007.
34. Werner HM, Trovik J, Halle MK, Wik E, Akslen LA, Birkeland E, Bredholt T, Tangen IL, Krakstad C and Salvesen HB: Stathmin protein level, a potential predictive marker for taxane treatment response in endometrial cancer. PLoS One 9: e90141, 2014.
35. Gache V, Louwagie M, Garin J, Caudron N, Lafanechere L and Valiron O: Identification of proteins binding the native tubulin dimer. Biochem Biophys Res Commun 327: 35-42, 2005.